The Astrophysical Journal, 593:571–580, 2003 August 10

DECIMETRIC SPIKE BURSTS VERSUS MICROWAVE CONTINUUM

Gregory D. Fleishman,[1,2,3] Dale E. Gary,[2] and Gelu M. Nita[2]
Received 2003 March 6; accepted 2003 April 16

ABSTRACT

We analyze properties of decimetric spike bursts occurring simultaneously with microwave gyrosynchrotron continuum bursts. We found that all of the accompanying microwave bursts were highly polarized in the optically thin range. The sense of polarization of the spike clusters is typically the same as that of the optically thin gyrosynchrotron emission, implying preferential extraordinary wave–mode spike polarization. Optically thick spectral indices of the continuum in spike-producing events were not observed to be larger than 2.5, suggesting low or absent Razin suppression. This implies that the plasma frequency–to-gyrofrequency ratio is systematically lower in the spike-producing bursts than in other bursts. The spike cluster flux density is found to be tightly correlated with the high-frequency spectral index of the microwave continuum for each event, while the flux-to-flux correlation may not be present. We discovered strong evidence that the trapped fast electrons producing the microwave gyrosynchrotron continuum have an anisotropic pitch-angle distribution of the loss cone type in the spike-producing bursts. The spike clusters are mainly generated when the trapped electrons have the hardest and the most anisotropic distributions. The new properties are discussed against the currently available ideas about emission processes and models for spike generation. We conclude that the findings strongly support the electron cyclotron maser mechanism of spike emission, with characteristics agreeing with expectations from the local-trap model.

Subject headings: acceleration of particles — Sun: flares — Sun: particle emission — Sun: radio radiation

1. INTRODUCTION

Millisecond solar radio spikes represent an interesting class of solar radio emission associated with flares. The spikes usually form a cluster of short-duration narrowband pulses on the dynamic spectrum, covering a range of about a few hundred MHz and lasting about a few minutes. This type of radio emission was initially interpreted as a signature of highly fragmented energy release in flares (Benz 1985). This idea had been one of the main "drivers" of the extensive observational (Benz, Zlobec, & Jaeggi 1982; Karlický 1984; Messerotti, Nonino, & Zlobec 1985; Stähli & Magun 1986; Benz & Güdel 1987; Güdel 1990; Gary, Hurford, & Flees 1991; Güdel, Aschwanden, & Benz 1991; Csillaghy & Benz 1993; Altyntsev et al. 1995, 1996; Karlický, Sobotka, & Jiřička 1996; Zlobec & Karlický 1998; Messmer & Benz 2000; Wang, Yan, & Fu 2002) and theoretical (Stepanov 1978; Kuijpers, van der Post, & Slottje 1981; Sharma, Vlahos, & Papadopoulos 1982; Sharma & Vlahos 1984; Li 1986; Winglee & Dulk 1986; Li 1987; Winglee, Dulk, & Pritchett 1988; Aschwanden 1990; Fleishman 1994; Fleishman & Yastrebov 1994b; Ledenev 1998; Stupp 2000; Bárta & Karlický 2001; Vlasov, Kuznetsov, & Altyntsev 2002) studies of the subject.

However, the integrated spike flux was found to be delayed by 2–5 s with respect to simultaneous hard X-ray (HXR) peaks (Aschwanden & Güdel 1992). This discovery is entirely inconsistent with the interpretation of the radio spikes as tracers of the primary energy release. Such a delay can be consistently explained in terms of spectral hardening of the respective fast electrons trapped in a coronal magnetic loop (Fleishman & Melnikov 1998). This model associates the appearance of the spikes with a secondary fragmentation of the radio source (related, e.g., to the local inhomogeneities of the magnetic field).

Another important driver for the spike study is the strong diagnostic potential of the spikes related, e.g., to their extremely narrow bandwidth and short duration (Benz 1986). As a result, many important properties of the spikes have been established from the analysis of observations, leading to the development of many models. Currently, the most detailed comparison of the observed spike properties with various theoretical models is done in a recent review paper (Fleishman & Melnikov 1998). It was shown that the complete list of spike properties can be interpreted within electron cyclotron maser (ECM) emission produced by fast electrons (with $E_{\rm kin} \sim 10$–100 keV) with a power-law momentum and anisotropic (loss cone) pitch-angle distributions. The source of a spike cluster is shown to be a loop with more or less strong local inhomogeneities forming some local traps, where the pitch-angle anisotropy is stronger than on average and provides strong local wave amplification as a result of negative gyrosynchrotron absorption. Thus, each local trap forms a site where a single spike is generated.

The model has since been developed further to account for some specific spike properties. For example, quasi-linear saturation of ECM (Fleishman & Arzner 2000) was shown to provide spike time profiles with a Gaussian rise phase and exponential decay phase, in agreement with spike observations (Güdel & Benz 1990; Fleishman & Melnikov 1998; Mészárosová et al. 2002). Noninteger harmonic ratios of the spikes (Krucker & Benz 1994) were interpreted as resulting from an ECM line splitting due to source inhomogeneity (Fleishman & Platonov 1999; Platonov & Fleishman 2001).

[1] Purple Mountain Observatory, National Astronomical Observatories, Nanjing 210008, China.
[2] New Jersey Institute of Technology, Newark, NJ 07102.
[3] Ioffe Institute for Physics and Technology, St. Petersburg 194021, Russia.

Nevertheless, in spite of the success of current models based on the ECM mechanism, the interpretation remains rather indirect; thus, more direct evidence for ECM operation in the spike bursts is strongly required.

According to ECM theory (Sharma et al. 1982; Sharma & Vlahos 1984; Li 1986; Winglee & Dulk 1986; Li 1987; Aschwanden 1990; Fleishman & Yastrebov 1994a; Fleishman & Melnikov 1998; Stupp 2000), this mechanism is effective if

1. the gyrofrequency to plasma frequency ratio is sufficiently large,

$$\omega_{\rm Be}/\omega_{\rm pe} \gtrsim 1 \; ; \qquad (1)$$

2. the distribution function of fast electrons over momentum is sufficiently hard, in the range of tens to hundreds of keV; and
3. the pitch-angle distribution of fast electrons is anisotropic (say, of the loss cone type).

There are various scenarios of ECM operation in solar flares. One of the widely accepted ideas assumes that the main population of fast electrons trapped in a loop is isotropic, while a minor fraction of the electrons just reflected up at the footpoints forms the loss cone distribution providing the cyclotron instability. Therefore, these models predict that the spikes are generated in a restricted area around the footpoints.

We envision another possibility. If the main electron distribution has an anisotropic pitch-angle distribution (close to marginal stability state), then fluctuations of the angular distribution can provide ECM emission at any location through the entire loop. This model allows spikes to be generated at any height. Moreover, the overall anisotropy will substantially affect the accompanying incoherent gyrosynchrotron emission (Fleishman & Melnikov 2003), which can be tested observationally.

In particular, the model developed by Fleishman & Melnikov (1998) assumes that the spikes are generated by a population of fast electrons accumulated in a magnetic loop because of formation of small-scale traps by inhomogeneities of the magnetic field. Gyrosynchrotron continuum bursts are known to be produced by trapped electrons as well (with characteristic electron energies from hundreds of keV to a few MeV).

Thus, the microwave continuum and simultaneous spike bursts should be related to each other. Since the properties of the gyrosynchrotron emission and its relation to the source parameters and fast-electron distribution are well known, we expect that analysis of some important correlations between spike bursts and gyrosynchrotron bursts might be rather informative to the study of solar radio spikes.

The study of spike cluster–to–microwave continuum correlations performed in this paper is similar, to some extent, to that done by Aschwanden & Güdel (1992), who considered the correlations between spike clusters and HXR emission. Unlike that study, however, we pay particular attention to the spectral properties of the microwave bursts (rather than flux-to-flux correlations only) and their association with energetic and pitch-angle distributions of the trapped fast electrons.

While both HXR and microwave emissions are produced by accelerated electrons with incoherent emission mechanisms, we emphasize that the study of spike-to-microwave correlations is not a simple repetition of the previous spike-to-HXR study, for a few reasons. HXRs are produced mainly by precipitating electrons, while gyrosynchrotron emission is by trapped electrons. Thus, these are different (while related) populations of accelerated electrons. Also, the characteristic energies of radiating electrons are different for these two emission types. And finally, the gyrosynchrotron emission is sensitive to the coronal magnetic field and plasma density, unlike HXR emission.

We found that all of the conditions required for ECM generation are fulfilled in the analyzed spike events, which is strong evidence that the spikes are produced by the ECM mechanism. Thus, the spike emission can be further used for more reliable diagnostics of the source parameters. In particular, we conclude that the spike clusters are associated with the flares that have the largest magnetic field (more specifically, the largest $\omega_{\rm Be}/\omega_{\rm pe}$ ratio).

The paper is arranged as follows. Section 2 discusses briefly the observations and selection criteria. Section 3 considers the theoretical concepts to be checked against the observations. Section 4 analyzes in some detail a few spike events recorded by the Owens Valley Solar Array (OVSA) during 2001. Finally, the results are discussed in § 5.

2. OBSERVATIONS

The OVSA (Hurford, Read, & Zirin 1984; Gary & Hurford 1994) observes in the frequency range 1–18 GHz, typically with 40 frequency channels. The standard temporal resolution is 4 s for the total intensity and 8 s for the circular polarization. The temporal resolution is obviously insufficient to resolve any single spike, since the typical spike duration is of the order of 10 ms or less in the frequency range 1–3 GHz (Güdel & Benz 1990; Mészárosová et al. 2002; Wang et al. 2002). Nevertheless, an averaged flux of a dense spike cluster can be observed with the OVSA resolution. The results we describe here pertain to average properties of such spike clusters. In particular, the average spike flux densities likely relate more closely to the spike occurrence rate than to individual spike flux densities (Aschwanden & Güdel 1992).

For the detailed analysis we selected a few events demonstrating fluctuating low-frequency (1–3.4 GHz) emission with timescales much less than the timescales of the simultaneous microwave continuum. Only the events with narrowband decimetric structures and without any indication of drifting structures (such as could be related to type III bursts) were selected. Also, we did not include the events with very few decimetric peaks, since no quantitative analysis was possible for those cases. Finally, we selected six events (from about 10 spike events recorded for the entire year 2001). Five of them were observed with the standard 4 and 8 s time resolution, while the sixth was with 2 s time resolution and without polarization measurements.

3. THEORETICAL BACKGROUND

In essence, ECM is a kind of gyrosynchrotron emission in which the absorption coefficient is negative, providing wave amplification instead of absorption. The usual solution for

the radiation intensity applies in this case (for a uniform source):

$$J_\sigma(\omega,\vartheta)=\frac{j_\sigma(\omega,\vartheta)}{\varkappa_\sigma(\omega,\vartheta)}(1-e^{-\tau_\sigma})\ , \tag{2}$$

where $\tau_\sigma=\varkappa_\sigma L$ is the optical depth of the source for either ordinary ($\sigma=1$) or extraordinary ($\sigma=-1$) modes of radiation, L is the source size along the line of sight, and $j_\sigma(\omega,\vartheta)$, $\varkappa_\sigma(\omega,\vartheta)$ are the emissivity and absorption coefficients of the gyrosynchrotron emission at frequency ω and viewing angle ϑ.

If the optical depth $|\tau|$ is large in value and positive, we arrive at the standard optically thick gyrosynchrotron emission, with the intensity

$$J_\sigma^{\rm thick}(\omega,\vartheta)=\frac{j_\sigma(\omega,\vartheta)}{\varkappa_\sigma(\omega,\vartheta)}\ , \tag{3}$$

whose spectral behavior does not depend noticeably on the electron spectral index.

However, if the absorption coefficient is negative for some restricted range of the frequency and viewing angle for any wave mode, the amplification of the respective waves occurs according to equation (2), which reduces to

$$J_\sigma^{\rm ECM}(\omega,\vartheta)=\frac{j_\sigma(\omega,\vartheta)}{|\varkappa_\sigma(\omega,\vartheta)|}e^{|\tau_\sigma|} \tag{4}$$

if $|\tau_\sigma|\gg 1$ for this case (in the linear approximation).

From these two equations it becomes very clear what kind of correlation should exist in observations when we compare ECM emission with the standard gyrosynchrotron emission. The ratio of the two becomes

$$\frac{J_\sigma^{\rm ECM}(\omega_1,\vartheta)}{J_\sigma^{\rm thick}(\omega_2,\vartheta)}=\frac{j_\sigma(\omega_1,\vartheta)/|\varkappa_\sigma(\omega_1,\vartheta)|}{j_\sigma(\omega_2,\vartheta)/\varkappa_\sigma(\omega_2,\vartheta)}e^{|\tau_\sigma|}\ , \tag{5}$$

where ω_1 is the (low) frequency at which ECM emission is generated, ω_2 is a (higher) frequency at which the gyrosynchrotron source is optically thick, and $|\tau_\sigma|$ is the optical depth of the ECM emission. The ratio depends primarily on the exponential factor $e^{|\tau_\sigma|}$, while the pre-exponential factor has a much weaker dependence on the distribution function of fast electrons (Fleishman & Melnikov 2003). Thus, the logarithm of the ratio (eq. [5]) is linearly related to the optical depth $|\tau_\sigma|$, which in turn depends substantially on the distribution function of fast electrons.

More specifically (Fleishman & Yastrebov 1994a; Fleishman & Melnikov 1998), the negative absorption coefficient (and hence $|\tau_\sigma|$) increases in value as the hardness of the electron momentum spectrum and pitch-angle anisotropy (namely, the angular gradient) of the loss cone distribution increase. On the other hand, the hardness and the pitch-angle distribution specify the optically thin spectral index of the incoherent gyrosynchrotron radiation (Ramaty 1969; Fleishman & Melnikov 2003).

The calculations of the standard gyrosynchrotron emission produced by anisotropic pitch-angle distributions of fast electrons with a power-law momentum distribution (Fleishman & Melnikov 2003) show that the optically thin spectral index (α_h) of the gyrosynchrotron radiation depends substantially on the viewing angle at which the gyrosynchrotron source is observed with respect to the magnetic field. For the quasi-transverse case, the spectral index is specified primarily by the spectral index δ of the fast-electron distribution over momentum, so that harder electron distributions produce flatter gyrosynchrotron spectra in the optically thin region. However, for the quasi-parallel case (Fleishman & Melnikov 2003), the spectral index α_h is specified mainly by the pitch-angle anisotropy of fast electrons in such a way that more anisotropic distributions produce softer optically thin gyrosynchrotron spectra (larger α_h).

Thus, combining the predictions of the ECM and gyrosynchrotron theories, we can expect two different types of correlation between $|\tau_\sigma|$ and α_h. If we observe the microwave source at a quasi-transverse direction, then the larger optical depth $|\tau_\sigma|$ should correspond to a flatter gyrosynchrotron spectrum in the optically thin region, while for the quasi-parallel case, the larger optical depth $|\tau_\sigma|$ should correspond to a steeper gyrosynchrotron spectrum.

4. DATA ANALYSIS

Aschwanden & Güdel (1992) considered correlations between the decimetric spike rate, integrated over some frequency range, and HXR emission. In particular, they found that some X-ray peaks are tightly correlated with the averaged spike flux density, while others are entirely uncorrelated. This was interpreted (but not proved) as a result of particle acceleration in different loops with only some (one) of them satisfying the specific conditions for the spike generation. Another important finding is a considerable time delay (of 2–5 s) of the averaged spike flux in respect to HXR peaks.

Accordingly, we performed some studies similar (and complementary) to those by Aschwanden & Güdel (1992), but we paid more attention to the role of gyrosynchrotron spectral evolution, based on the theoretical concepts discussed briefly in § 3.

First of all, we address the question of whether there are any indications that the ratio of frequencies (eq. [1]) is systematically larger for bursts producing the spike clusters than on average for all radio bursts. For this purpose we study the low-frequency part of the microwave continuum bursts. It is well known (Bastian, Benz, & Gary 1998; Fleishman & Melnikov 2003) that the slope (α_l) of the low-frequency gyrosynchrotron emission depends on the gyrofrequency-to–plasma frequency ratio because of the Razin effect. While the expected low-frequency spectral indices for the gyrosynchrotron optical depth is $\alpha_l<3$, the Razin effect can increase the values to the range $\alpha_l>3$ if $\omega_{\rm Be}/\omega_{\rm pe}<0.3$.

Figure 1 displays the distributions of the low-frequency spectral indices α_l separately for the spike-producing bursts and all other gyrosynchrotron bursts. It is remarkable that the overall distribution has a significant tail in the range $\alpha_l>3$, while the spike-producing bursts display spectral indices lying entirely in the range $\alpha_l<2.5$. Thus, no indication of the Razin effect operating in the spike-producing bursts is present; hence, we can conclude that the condition 1 (eq. [1]) is fulfilled for these events.

Below we analyze in more detail the six events with dense spike clusters in the range 1.2–3.4 GHz recorded by OVSA during 2001.

4.1. *2001 March 25 Event*

The event lasted about 8 minutes (Fig. 2*a*), and the microwave continuum burst produced a flux density of up to 50 sfu, while the decimetric flux density exceeded 150 sfu.

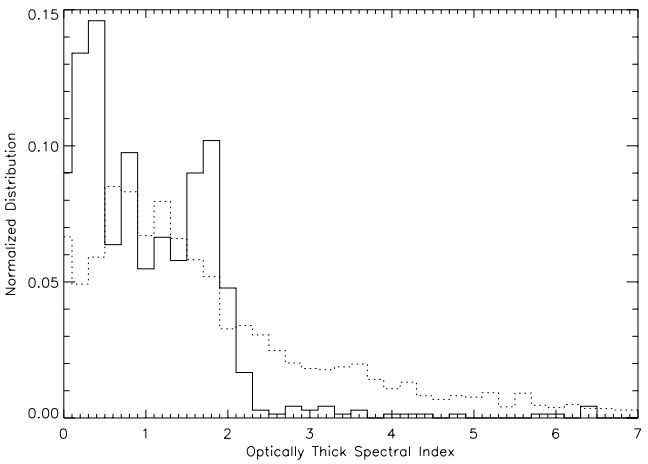

FIG. 1.—Distribution of optically thick spectral index of six spike-producing bursts (*solid line*) and the equivalent distribution obtained for 125 gyrosynchrotron bursts above 60 sfu (*dashed line*) observed by OVSA during 2001.

The power and polarization spectra, averaged over the entire burst duration, are shown in Figures 2*b* and 2*c*. The microwave burst displays a remarkably strong degree of polarization at the high (optically thin) frequencies. A few important conclusions can be derived from the polarization plot. First, the microwave source is reasonably uniform; otherwise, the degree of polarization might not have been so strong. Second, we look at the source at a direction quasi-parallel to the magnetic field, since at a quasi-transverse direction even a uniform source would produce a weak or moderate degree of polarization. Third, the dominant sense of circular polarization (left, or L) for the spikes is that expected for optically thin gyrosynchrotron emission (X-mode) and opposite to that of optically thick emission (typically, O-mode). Thus, the spikes are preferentially X-mode–polarized (within the simplest geometry). We have to emphasize that we discuss here an averaged degree of polarization of the entire spike cluster, while the instantaneous degree of polarization varies with time and can be as large as 100%. The sense of spike polarization also changes with time. Moreover, the preferential sense of spike polarization depends on frequency: lower frequency spikes (1.2–2 GHz) are mainly L-polarized, while higher frequency spikes (2–3.4 GHz) are mainly R-(right-circularly) polarized.

Let us proceed to examine correlations between spike emission and microwave continuum. Figure 3*a* displays a very good correlation between averaged spike flux and the microwave light curve. This finding is similar to that found for HXR bursts accompanied by spike clusters: some HXR peaks are tightly correlated with the spike rate (Aschwanden & Güdel 1992). Aschwanden & Güdel (1992) found that the averaged spike flux is delayed by 2–5 s with respect to the simultaneous HXR peak, which was further interpreted as a result of trapping and consequent spectral evolution of spike-generating fast electrons (Fleishman & Melnikov 1998), while the HXR peak is caused mainly by precipitating electrons.

Figure 3*b* displays the dependence of the cross-correlation coefficient between the spike flux density integrated over the low-frequency band and the gyrosynchrotron flux density at a selected (optically thick)

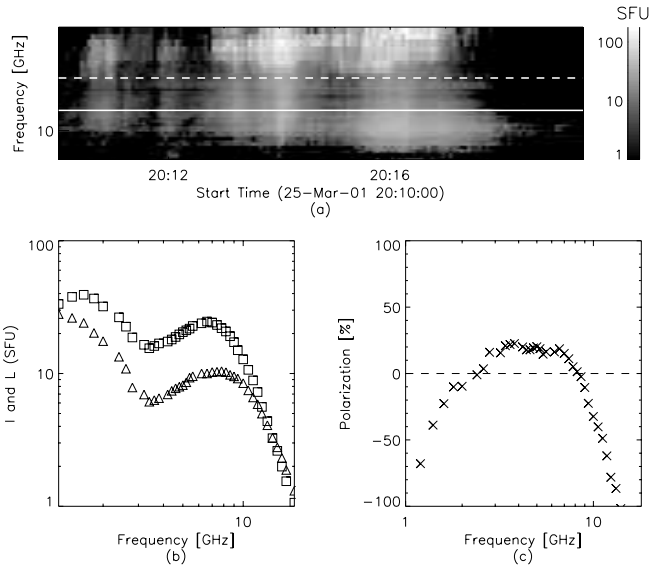

FIG. 2.—2001 March 25. (*a*) Dynamic spectrum recorded by OVSA at 40 frequencies between 1.2 and 18 GHz at 4 s time resolution. The solid line, 6.6 GHz, and the dashed line, 3.4 GHz, represent, respectively, the optically thick frequency and the upper integration limit of the spiky emission used to obtain the results displayed in Fig. 3. (*b*) Time-averaged total power emission (*squares*) and L-polarization data (*triangles*) for the same segment of time as in (*a*). (c) Averaged polarization spectrum computed using the magnitudes displayed in (*b*).

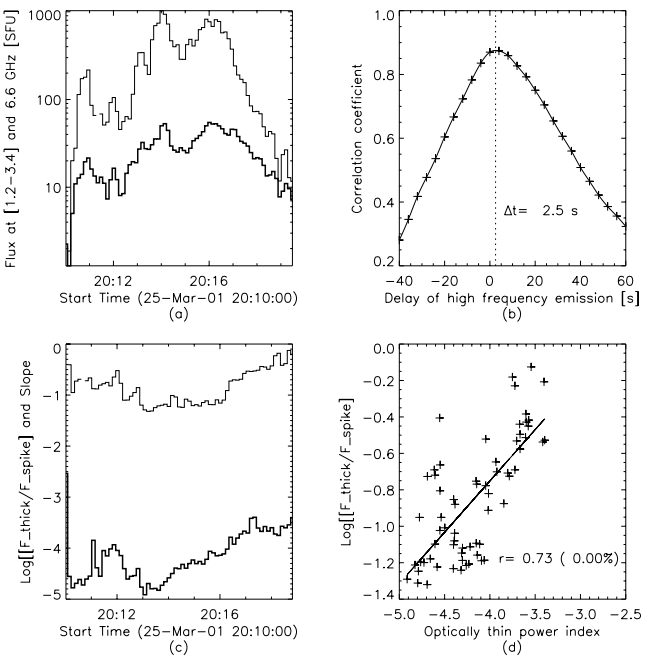

FIG. 3.—2001 March 25. (*a*) Integrated spiky emission over 1.2–3.4 GHz (*thin line*) and the optically thick gyrosynchrotron emission at 6.6 GHz (*thick line*). (*b*) Linear correlation coefficient (*symbols*) between the magnitudes displayed in (*a*) for different time lags. A delay of 2.5 s for the high-frequency emission relative to the integrated low-frequency emission has been estimated using a spline interpolation (*solid line*). (*c*) Natural logarithm of the ratio between optically thick and integrated spiky emissions (*thin line*) and the optically thin spectral index (*thick line*). (*d*) Correlation plot of the magnitudes displayed in (*c*). A linear correlation coefficient of +0.73 has been found. The probability for such a correlation coefficient to be the result of a random distribution is 0% to two decimal places.

frequency as a function of the respective time lag. The corresponding spline fit (*solid curve*) has a maximum at $\Delta t \approx 2.5$ s; accordingly, the *optically thick* gyrosynchrotron emission is delayed by 2.5 s with respect to the spike emission. Indeed, the delay value is frequency-dependent, in agreement with the property of the microwave bursts (Melnikov & Magun 1998), but the sign is stable. Since both types of radio emission are produced by trapped electrons, the delay can be easily interpreted if the spike emission is produced by fast electrons of lower energy than the gyrosynchrotron emission, because the characteristic lifetime of the trapped electrons increases with the electron energy.

The theory described in § 3 predicts a correlation between the (negative) optical depth in the spike frequency range and the gyrosynchrotron spectral index α_h in the optically thin range. To study this correlation, we plot in Figure 3*c* the quantity $\log\left(F_{\rm thick}/F_{\rm spike}\right)$ versus the high-frequency microwave spectral index α_h, where $F_{\rm thick}$ is the gyrosynchrotron flux density at an optically thick frequency, namely, $f = 6.6$ GHz, and $F_{\rm spike}$ is the spike flux density integrated from 1.2 to 3.4 GHz. The corresponding correlation coefficient is remarkably large, $R = 0.73$. The positive slope of the regression means that spikes are preferentially generated when the optically thin gyrosynchrotron emission displays the softest spectrum, which (for the quasi-parallel viewing angle) corresponds to the most anisotropic pitch-angle distributions of the fast electrons.

4.2. *2001 August 24 Event*

The event shown in Figure 4*a* is generally similar to the previous one but an order of magnitude stronger: the microwave peak flux is about 400 sfu, while the spike peak flux density is about 1500 sfu. The total and polarized flux densities (Fig. 4*b*) give rise to the averaged polarization spectrum shown in Figure 4*c*. The degree of polarization is exceedingly strong at the high (optically thin) frequencies, which is evidence for the quasi-parallel viewing angle of the

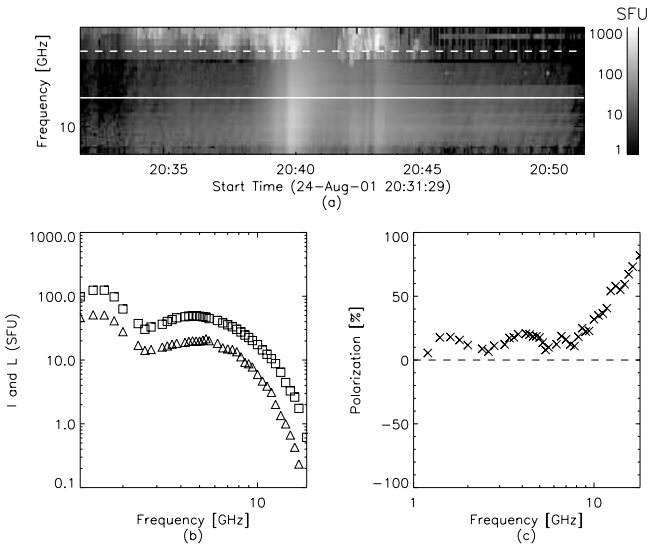

FIG. 4.—2001 August 24. (*a*) Dynamic spectrum recorded by OVSA at 40 frequencies between 1.2 and 18 GHz at 4 s time resolution. The solid line, 5.4 GHz, and the dashed line, 2.0 GHz, represent, respectively, the optically thick frequency and the upper integration limit of the spiky emission used to obtain the results displayed in Fig. 5. (*b*) Same as Fig. 2*b*. (*c*) Same as Fig. 2*c*.

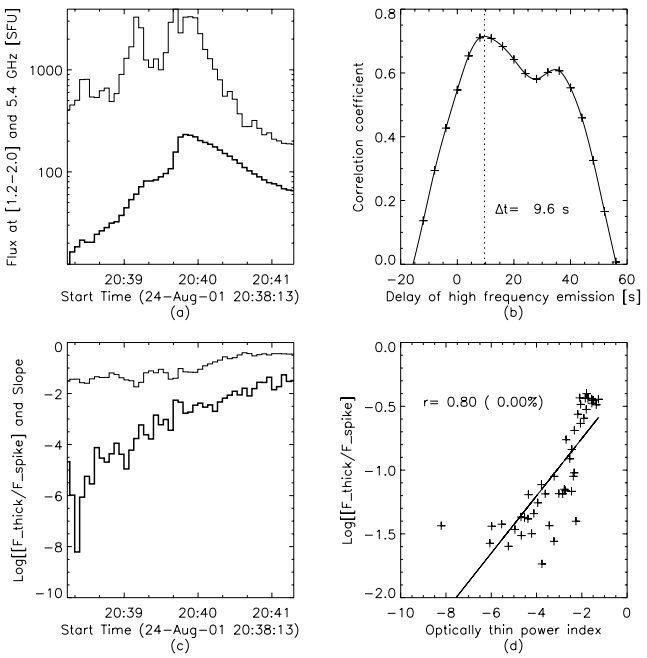

FIG. 5.—2001 August 24. (*a*) Integrated spiky emission over 1.2–2.0 GHz (*thin line*) and the optically thick gyrosynchrotron emission at 5.4 GHz (*thick line*). (*b*) Same as Fig. 3*b*. The estimated delay for the high-frequency emission is 9.6 s. (*c*) Same as Fig. 3*c*. (*d*) Correlation plot of the magnitudes displayed in (*c*). A linear correlation coefficient of +0.80 has been found. The probability for such a correlation coefficient to be the result of a random distribution is again 0%.

gyrosynchrotron source. It is interesting that the sense of polarization in the optically thick region is the same as in the optically thin region, which can be naturally interpreted as an effect of pitch-angle anisotropy of the radiating fast electrons (Fleishman & Melnikov 2003). The spikes are mainly polarized with the same sense; thus, we again arrive at the conclusion of the preferential X-mode polarization of the spikes.

The averaged spike and microwave fluxes display a significant correlation (Fig. 5*a*), with a correlation coefficient $R = 0.72$. The microwave emission is delayed by about 9.6 s with respect to the spike emission (Fig. 5*b*), which again is expected because of the energy-dependent lifetime of the trapped fast electrons.

The logarithm of the ratio of the optically thick gyrosynchrotron flux density to the averaged spike flux density (Fig. 5*c*) displays an especially tight correlation with the high-frequency microwave spectral index (Fig. 5*d*) during a 3 minute interval of the burst (from 20:38:10 to 20:41:20 UT), when reliable spectral index data are available. Thus, we again conclude that the spikes are mainly generated during the softest microwave spectra. For the quasi-parallel case, softer spectra indicate more anisotropic pitch-angle distributions of the fast electrons; hence, the spikes are produced most efficiently when the pitch-angle distribution of the trapped fast electrons is the most anisotropic.

4.3. *2001 August 30 Event*

The event lasted about 10 minutes (Fig. 6*a*), but only the main phase (from 17:49:30 to 17:53:00 UT) allows for the quantitative analysis requiring data of sufficiently high flux density. The peak flux densities of both microwave and

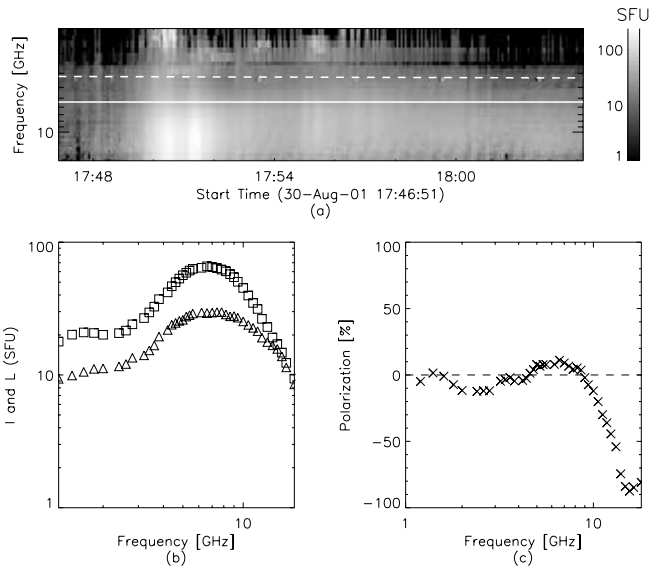

FIG. 6.—2001 August 30. (*a*) Dynamic spectrum recorded by OVSA at 40 frequencies between 1.2 and 18 GHz at 4 s time resolution. The solid line, 5.4 GHz, and the dashed line, 3.2 GHz, represent, respectively, the optically thick frequency and the upper integration limit of the spiky emission used to obtain the results displayed in Fig. 7. (*b*) Same as Fig. 2*b*. (*c*) Same as Fig. 2*c*.

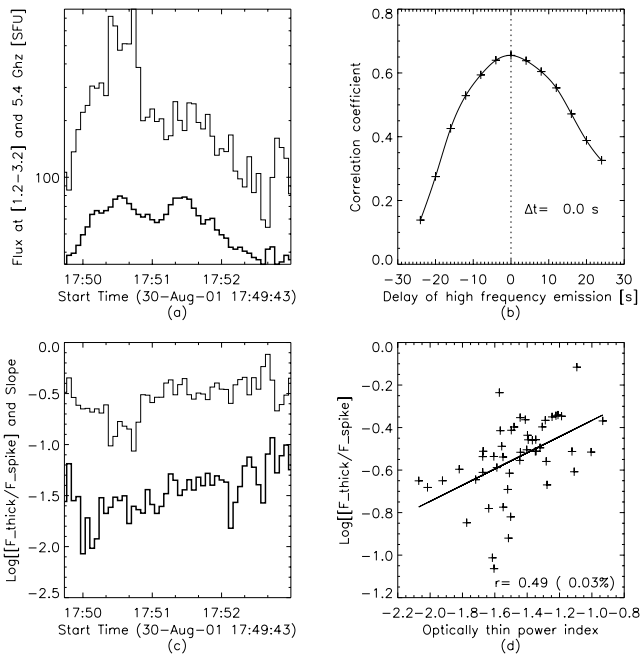

FIG. 7.—2001 August 30. (*a*) Integrated spiky emission over 1.2–3.2 GHz (*thin line*) and the optically thick gyrosynchrotron emission at 5.4 GHz (*thick line*). (*b*) Same as Fig. 3*b*. Practically no delay between high-frequency emission and the integrated low-frequency emission has been found in this case. (*c*) Same as Fig. 3*c*. (*d*) Correlation plot of the magnitudes displayed in (*c*). A linear correlation coefficient of +0.49 has been found. The probability for such a correlation coefficient to be the result of a random distribution is about 0.03%.

spike emissions exceed 200 sfu in this event. The spikes display clustering in the frequency domain; we analyze here the properties of the spike flux integrated over the entire range from 1.2 to 3.2 GHz. The averaged total and polarized flux densities (Fig. 6*b*) provide us with the polarization spectrum (Fig. 6*c*). The very large degree of polarization in the optically thin range allows us to derive that the microwave source is observed at a direction quasi-parallel to the magnetic field, similar to that in the previous two cases. The sense of polarization of the spike clusters is the same as that of the optically thin gyrosynchrotron emission, once again suggesting the preferential X-mode polarization of spikes.

The first microwave peak is well correlated with the integrated spike flux, while the second one displays a much weaker correlation, similar the findings of the spike-HXR correlation study (Aschwanden & Güdel 1992). For this reason, the flux-to-flux correlation is not quite so strong ($R = 0.66$) for the entire analyzed time segment (Fig. 7*a*). The dependence of the correlation coefficient of the time lag (Fig. 7*b*) shows that the microwave emission is delayed only slightly, if at all, with respect to the spike emission.

The correlation between $\log\left(F_{\rm thick}/F_{\rm spike}\right)$ and α_h remains significant, at $R = 0.49$, but is less than in the two previous cases. Nevertheless, the general conclusion is the same for all three analyzed events, demonstrating strong polarization of the optically thin gyrosynchrotron emission: the spikes are generated most efficiently when the gyrosynchrotron emission displays the softest spectra.

4.4. *2001 October 5 Event*

The spikes in this event lasted about 6 minutes (Fig. 8*a*). This is the weakest of the analyzed events, the peak flux density of both microwave and spike bursts being below 100 sfu (Fig. 8*b*).

The total and polarized flux data are reliable at $f < 10$ GHz (Fig. 8*b*), above which the flux density becomes too low. The polarization spectrum displays a moderate degree of polarization ($P < 50\%$) in the optically thin region (Fig. 8*c*). In essence, there are a few possibilities to provide such a moderate polarization of the gyrosynchrotron emission

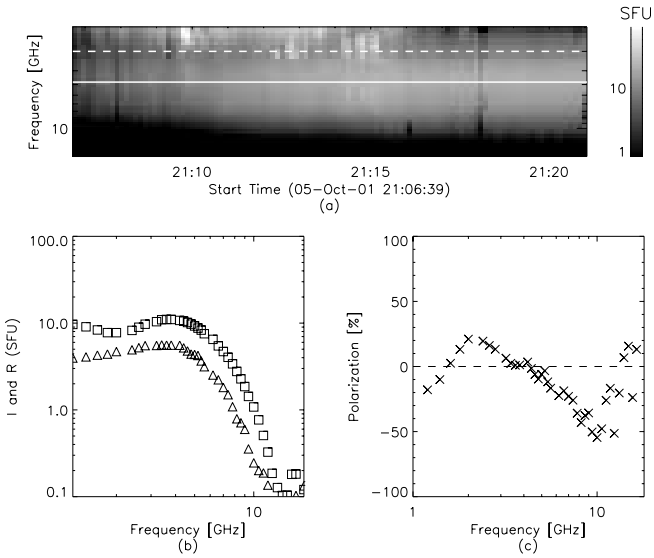

FIG. 8.—2001 October 5. (*a*) Dynamic spectrum recorded by OVSA at 40 frequencies between 1.2 and 18 GHz at 8 s time resolution. The solid line, 3.8 GHz, and the dashed line, 2.0 GHz, represent, respectively, the optically thick frequency and the upper integration limit of the spiky emission used to obtain the results displayed in Fig. 9. (*b*) Time-averaged total power emission (*squares*) and R-polarization data (*triangles*) for the same segment of time as in (*a*). (*c*) Same as Fig. 2*c*. Only the polarization spectrum below 10 GHz is reliable because of the very weak emission above this frequency, as can be seen in (*b*).

(e.g., a single source observed at a quasi-transverse direction, superposition of two quasi-parallel sources with opposite directions of the magnetic field, or a more complicated nonuniform source).

However, we adopt the simplest model—a single gyrosynchrotron source—as we did for the three previous events. In this case, the source is observed at a quasi-transverse direction (to avoid very strong high-frequency polarization). One can note that the spikes above 1.6 GHz are polarized oppositely to the optically thin gyrosynchrotron emission, while below 1.6 GHz they have the same sense of polarization.

The averaged spike and microwave fluxes display a rather small correlation coefficient, $R = 0.13$ (Fig. 9*b*), although there is some indication that the microwave emission is delayed by 5.9 s with respect to the spike emission (Fig. 9*b*). Nevertheless, the quantities $\log\left(F_{\rm thick}/F_{\rm spike}\right)$ and α_h reveal a significant negative correlation, $R = -0.46$ (Fig. 9*d*), implying a physical relation between these two emission types. The negative slope of the regression means that the spikes are generated most efficiently when the gyrosynchrotron emission displays the hardest spectra, in contrast to the three previous bursts.

For the quasi-transverse viewing angles, the high-frequency slope is related primarily to the hardness of the fast electron momentum distribution. We, thus, conclude that the spikes are generated when the fast electrons have the hardest spectrum. A similar property was noted in the spike-HXR correlation study (Aschwanden & Güdel 1992).

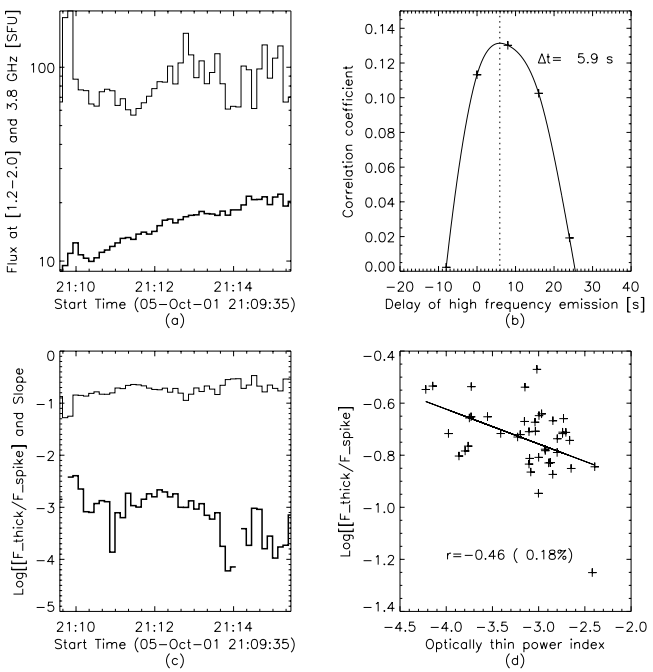

FIG. 9.—2001 October 5. (*a*) Integrated spiky emission over 1.2–2.0 GHz (*thin line*) and the optically thick gyrosynchrotron emission at 3.8 GHz (*thick line*). (*b*) Same as Fig. 3*b*. The estimated delay for the high-frequency emission is 5.9 s. (*c*) Same as Fig. 3*c*. (*d*) Correlation plot of the magnitudes displayed in (*c*). A linear correlation coefficient of −0.46 has been found. The probability for such a correlation coefficient to be the result of a random distribution is about 0.18%.

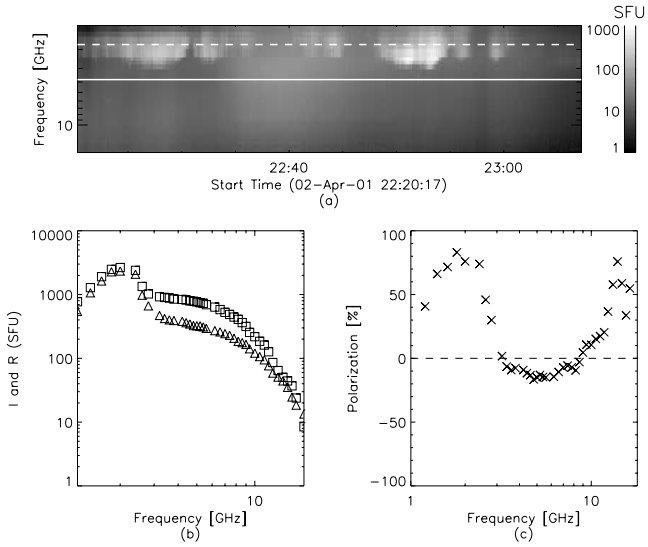

FIG. 10.—2001 April 2. (*a*) Dynamic spectrum recorded by OVSA at 40 frequencies between 1.2 and 18 GHz and 4 s time resolution. The solid line, 3.8 GHz, and the dashed line, 1.8 GHz, represent, respectively, the optically thick frequency and the upper integration limit of the spiky emission used to obtain the results displayed in Fig. 11. (*b*) Same as Fig. 8*b*. (*c*) Same as Fig. 2*c*.

4.5. *2001 April 2 Event*

This event (Fig. 10*a*) is exceptionally strong. The microwave peak exceeded 1000 sfu, while the spike flux exceeded 3×10^4 sfu. The event lasted more than half an hour and produced a few spike clusters. We analyze them all together, which provides a very long time series that improves the statistical significance of the results.

The polarization of the optically thin gyrosynchrotron emission (Fig. 10*c*) is moderate ($P < 60\%$), which is interpreted here (as the simplest assumption) as an effect of quasi-transverse viewing angle of the gyrosynchrotron source. The polarization of spike clusters is rather strong, $P \sim 70\%$–90% on average, and the sense of polarization is the same as for optically thin gyrosynchrotron emission. Thus, the spikes are preferentially X-mode–polarized.

The microwave and integrated spike fluxes are remarkably uncorrelated (Figs. 11*a* and 11*b*), at least on average (while some "tracks" can be noted in the plot). Accordingly, no delay between these two types of emission can be found reliably for this event.

However, if the spikes are produced by the ECM mechanism, the correlation between $\log\left(F_{\rm thick}/F_{\rm spike}\right)$ and α_h *must* exist. Figures 11*c* and 11*d* display this remarkable correlation ($R = -0.61$) related to the entire duration of the event (more than half an hour!). The spikes are again generated when the gyrosynchrotron emission displays the hardest spectra, which, for the quasi-transverse case, corresponds to the hardest spectra of the fast electrons.

4.6. *2001 October 19 Event*

This is one of the strongest events (Fig. 12) recorded in 2001: the microwave peak exceeded 5000 sfu, while the spike flux exceeded 3×10^4 sfu (Fig. 13*a*). The event was observed with a time resolution of 2 s, and we analyzed the period during the first peak (first ~7 minutes) of the event, during

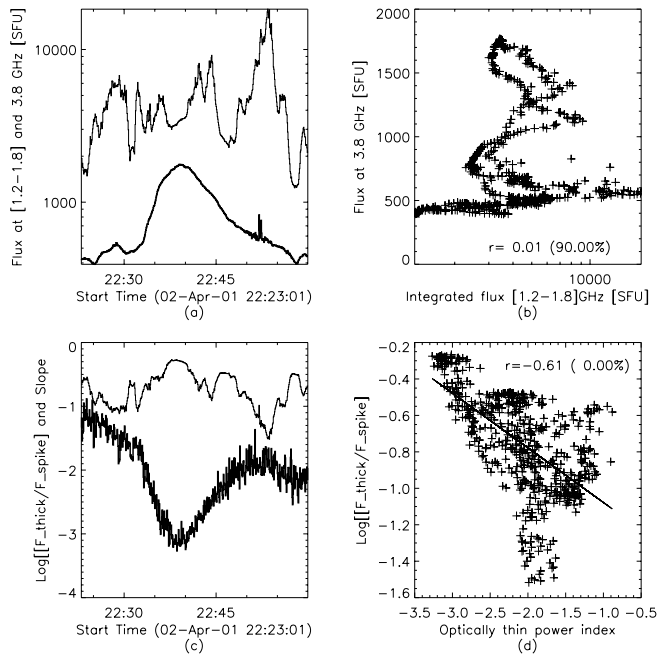

FIG. 11.—2001 April 2. (*a*) Integrated spiky emission over 1.2–1.8 GHz (*thin line*) and the optically thick gyrosynchrotron emission at 3.8 GHz (*thick line*). (*b*) Correlation plot of the magnitudes displayed in (*a*). No reliable delay could be found. For the case shown (no time lag), there is practically no linear correlation ($r = 0.01$, corresponding to a 90% probability of a random distribution). (*c*) Same as Fig. 3*c*. (*d*) Correlation plot of the magnitudes displayed in (*c*). A linear correlation coefficient of −0.61 has been found. The probability for such a correlation coefficient to be the result of a random distribution is 0% to two decimal places.

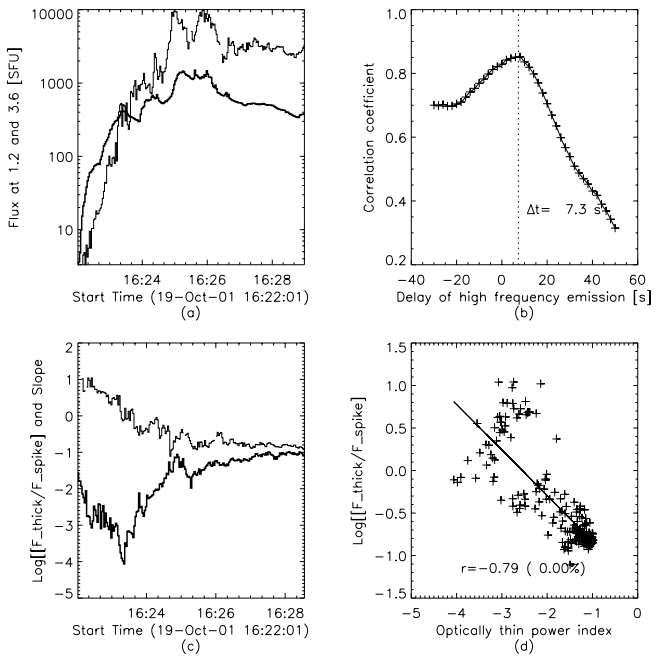

FIG. 13.—2001 October 19. (*a*) Emissions at 1.2 GHz (*thin line*) and the optically thick gyrosynchrotron emission at 3.6 GHz (*thick line*). (*b*) Same as Fig. 3*b*. The estimated delay for the high-frequency emission is 7.3 s. (*c*) Same as Fig. 3*c*. (*d*) Correlation plot of the magnitudes displayed in (*c*). A linear correlation coefficient of −0.79 has been found. The probability for such a correlation coefficient to be the result of a random distribution is again 0%.

which the spikes were obviously stronger than the competing low-frequency continuum emission.

The polarization data are unavailable with the fast mode; thus, we are limited to the total flux data for this event. There is general flux-to-flux correspondence for this case (Fig. 13*a*), providing a correlation of $R = 0.85$ (Fig. 13*b*). The microwave emission is delayed by 7.3 s with respect to the spike flux at $f = 1.2$ GHz. Unlike in the previous events, we did not integrate the decimetric flux over a few frequency channels, because the contribution of the smoothed decimetric continuum component becomes important at higher frequencies (1.4–2 GHz) during parts of the burst.

The correlation between $\log\left(F_{\rm thick}/F_{\rm spike}\right)$ and α_h is quite strong and negative for this case, $R = -0.79$ (Fig. 13*d*). We note that the correlation between $\log\left(F_{\rm thick}/F_{\rm spike}\right)$ and α_h remains negative until about halfway through the second gyrosynchrotron peak, at ∼1631 UT, and then reverses to a positive correlation, which we believe is due to the spike emission giving way to a low-frequency continuum emission of another origin. Although spike clusters appear later in the burst, the gyrosynchrotron emission peaks at such a low frequency after about 1640 UT that we cannot obtain the optically thick flux density and so cannot examine the correlation between $\log\left(F_{\rm thick}/F_{\rm spike}\right)$ and α_h. Therefore, at least during the first 7 minutes of this event, when the correlation can be performed, we can classify the event as being observed at a quasi-transverse direction, similarly to two previous events, and we once again conclude that harder electron distributions are preferable for the spike generation.

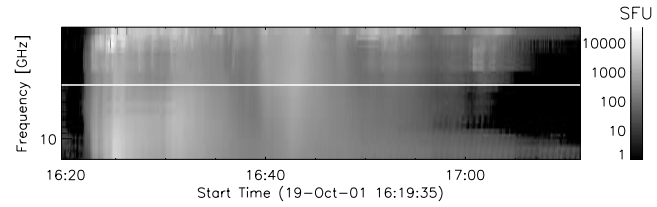

FIG. 12.—2001 October 19. Dynamic spectrum recorded by OVSA at 22 frequencies between 1.2 and 14.8 GHz and 2 s time resolution. The solid line, 3.6 GHz, represents the optically thick frequency used to obtain the results displayed in Fig. 13. To analyze the spiky emission, only one frequency, 1.2 GHz, has been used in this case, because a smoothed component becomes important for higher frequencies at the low frequency range. No polarization data are available for this event.

5. DISCUSSION

We analyzed in some detail six events producing dense spike clusters in the frequency range 1.2–3.4 GHz observed simultaneously with microwave gyrosynchrotron continuum.

A few new important findings are firmly established. First of all, the low-frequency part of the respective microwave bursts is considerably flatter than for the overall microwave event set. This means that there is no indication of the Razin effect operating in the microwave events accompanying the decimetric spike bursts. Consequently, the ratio $\omega_{\rm Be}/\omega_{\rm pe}$ is large enough in the spike sources to allow operation of the ECM mechanism.

Second, all five events with polarization data available reveal a *high* degree of polarization in the optically thin gyrosynchrotron range, significantly larger than typical

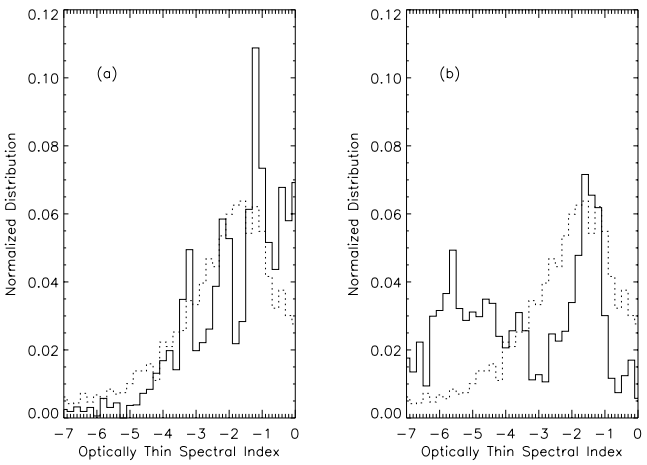

FIG. 14.—(*a*) Distribution of optically thin spectral index of the presumably quasi-transverse observed spike-producing bursts (*solid line*). (*b*) Same as (*a*), but for the presumably quasi-parallel observed spike-producing bursts (*solid line*). Both distributions are compared with that obtained for 125 gyrosynchrotron bursts above 60 sfu observed by OVSA during 2001 (*dashed lines*).

mean value of $20\% \pm 16\%$ (Bruggmann & Magun 1990). This deviation is most probably related to the fast-electron pitch-angle anisotropy (of the loss cone type), which increases the degree of X-mode polarization compared with the isotropic case (Fleishman & Melnikov 2003). Moreover, two of the analyzed events do not display a change of the sense of polarization from the thin to the thick region, which might be related to the effect of the pitch-angle anisotropy as well (Fleishman & Melnikov 2003). Note that the high degree of polarization implies a rather nonsymmetric magnetic structure at the source site, since a symmetric loop would give more equal fluxes in both polarizations, leading to smaller net polarization.

Third, important information about the pitch-angle anisotropy of the radiating fast electrons can be obtained from the analysis of the distribution of the high-frequency microwave spectral indices. Figure 14*a* displays the distribution of spectral indices for the quasi-transverse spike-producing bursts overplotted on the overall distribution for the gyrosynchrotron bursts above 60 sfu. The average hardness of spike-producing events is similar to that for all other events (however, one could note a lack of soft $\alpha_h < -3$ values for the spike-producing events). Since α_h is related to the fast-electron momentum distribution for the quasi-transverse case (Fleishman & Melnikov 2003), we can conclude that the spikes are produced by the electrons with a more or less typical energy spectrum. However, for the quasi-parallel case, the pitch-angle anisotropy can provide much softer gyrosynchrotron spectra for the same electron energy spectrum. Figure 14*b* displays the distribution of the spectral indices for the quasi-parallel spike-producing bursts overplotted on the overall distribution for the gyrosynchrotron bursts above 60 sfu. The respective gyrosynchrotron spectra are significantly softer than on average (one can note a strong excess in the range of $-7 < \alpha_h < -4$), which could only be ascribed to the effect of the pitch-angle anisotropy. This pitch-angle anisotropy is favorable to produce coherent ECM or plasma emission. However, the preferential X-mode polarization of the spikes, together with the variations of the sense of polarization observed in many events, is evidence of the ECM mechanism of spike production. The conclusion of the preferential X-mode polarization of the spikes agrees with the results of Güdel & Zlobec (1991). Since the ECM mechanism allows for both modes to be generated (Stupp 2000), the finding of Benz & Pianezzi (1997) that (for a selected set of spike observations) the original spikes are entirely O-mode–polarized at their source is consistent with this model as well.

Fourth, the analyzed events fall into two distinctive groups: those with a strong polarization of high-frequency gyrosynchrotron emission display a positive correlation between $\log\left(F_{\rm thick}/F_{\rm spike}\right)$ and α_h, while those with a weaker polarization display a negative (anti-)correlation between these two quantities. We interpret this difference as an effect of the viewing angle at which the gyrosynchrotron source is observed: strong polarization corresponds to a viewing angle quasi-parallel to the magnetic field, while weaker polarization corresponds to the quasi-transverse case. For the quasi-parallel case, the gyrosynchrotron spectral index depends primarily on the pitch-angle anisotropy (Fleishman & Melnikov 2003); namely, it increases as the anisotropy increases. However, for the quasi-transverse case, the effect of pitch-angle anisotropy on the spectral index is weak, and the spectral index is specified primarily by the electron energy distribution, as for isotropic case. This interpretation of these two kinds of the correlation plots is pretty consistent with the distributions of the high-frequency spectral indices (Fig. 14) discussed above.

From the entire set of data, we therefore conclude that the millisecond solar radio spikes are generated at a source with a relatively high gyrofrequency-to–plasma frequency ratio, during that phase of the bursts when the trapped fast electrons have the hardest energy distribution and the most anisotropic pitch-angle distribution. These properties are naturally expected within ECM theory (Fleishman & Yastrebov 1994a), while meeting large difficulties within alternative theories based on various modifications of the plasma mechanism (Fleishman & Melnikov 1998). Moreover, the pitch-angle anisotropy of the trapped electrons suggested by the data is in favor of the local-trap model (Fleishman & Melnikov 1998), while it is inconsistent with footpoint source models of spike generation.

The incoherent microwave emission is found to be delayed significantly (by 5–30 s) with respect to averaged spike flux density. Combining this finding with the result of Aschwanden & Güdel (1992) that the averaged spike flux is delayed by 2–5 s in respect to simultaneous HXR peaks, we conclude that HXR emission arrives first, then the spike emission, and finally the incoherent gyrosynchrotron emission. This sequence is related to underlying kinetics of fast electrons: the directly precipitating electrons produce HXR emission, low-energy trapped electrons produce spikes, and higher energy trapped electrons produce incoherent gyrosynchrotron emission. This is consistent with the delays (of a few seconds to a few tens of seconds) between HXR peaks and microwave bursts found earlier (Melnikov 1994).

Aschwanden & Güdel (1992) found that sometimes there is very tight correlation between the averaged spike flux and the respective HXR flux, but sometimes there is no good flux-to-flux correlation. We found here the same property when considering the microwave emission in place of HXR emission. However, *each* spike-producing burst reveals a significant correlation between $\log\left(F_{\rm thick}/F_{\rm spike}\right)$ and the high-frequency slope α_h of the microwave gyrosynchrotron

emission. This slope is related to the energy and pitch-angle distributions of the radiating fast electrons. We thus conclude that the spike production is directly related to the properties of the distribution function (over the momentum and pitch angle) of the trapped electrons.

The derived properties of the distribution functions, as well as source conditions (large ω_{Be}/ω_{pe} ratio), are found to be pretty consistent with those required for the ECM operation. We therefore can conclude that the performed study gives rise to new, important evidence that millisecond solar radio spikes are produced by the ECM mechanism.

Nevertheless, we feel that some important additional studies are necessary. For example, spatially resolved data are strongly desirable to locate the spike source with respect to the microwave source and the respective magnetic field. Also, the combined analysis of the spike, microwave, and HXR bursts observed for the same events can be exceedingly helpful to constrain the involved parameters and use the spike emission for further diagnostic purposes. From this point of view, some additional work should be done to specify the gyroharmonics providing the main contribution to the radio spike emission.

The work was supported by NSF grant AST 99-87366 and NASA grant NAG 5-11875 to New Jersey Institute of Technology, the Russian Foundation for Basic Research grants 02-02-39005 and 03-02-17218, and the Chinese NFS project 10273025 and " 973 " program grant G2000078403.

REFERENCES

Altyntsev, A. T., Grechnev, V. V., Konovalov, S. K., Lesovoi, S. V., Lisysian, E. G., Treskov, T. A., Rosenraukh, Yu. M., & Magun, A. 1996, ApJ, 469, 976
Altyntsev, A. T., Grechnev, V. V., Zubkova, G. N., Kardapolova, N. N., Lesovoi, S. V., Rosenraukh, Yu. M., & Treskov, T. A. 1995, A&A, 303, 249
Aschwanden, M. J. 1990, A&AS, 85, 1141
Aschwanden, M. J., & Güdel, M. 1992, ApJ, 401, 736
Bárta, M., & Karlický, M. 2001, A&A, 379, 1045
Bastian, T. S., Benz, A. O., & Gary, D. E. 1998, ARA&A, 36, 131
Benz, A. O. 1985, Sol. Phys., 96, 357
———. 1986, Sol. Phys., 104, 99
Benz, A. O., & Güdel, M. 1987, Sol. Phys., 111, 175
Benz, A. O., & Pianezzi, P. 1997, A&A, 323, 250
Benz, A. O., Zlobec, P., & Jaeggi, M. 1982, A&A, 109, 305
Bruggmann, G., & Magun, A. 1990, A&A, 239, 347
Csillaghy, A., & Benz, A. O. 1993, A&A, 274, 487
Fleishman, G. D. 1994, Sol. Phys., 153, 367
Fleishman, G. D., & Arzner, K. 2000, A&A, 358, 776
Fleishman, G. D., & Melnikov, V. F. 1998, Phys.–Uspekhi, 41, 1157
———. 2003, ApJ, 587, 823
Fleishman, G. D., & Platonov, K. Yu. 1999, in Magnetic Fields and Solar Processes, ed. A. Wilson (ESA SP-448; Noordwijk: ESA), 2, 809
Fleishman, G. D., & Yastrebov, S. G. 1994a, Sol. Phys., 153, 389
———. 1994b, Sol. Phys., 154, 361
Gary, D. E., & Hurford, G. J. 1994, ApJ, 420, 903
Gary, D. E., Hurford, G. J., & Flees, D. J. 1991, ApJ, 369, 255
Güdel, M. 1990, A&A, 239, L1
Güdel, M., Aschwanden, M. J., & Benz, A. O. 1991, A&A, 251, 285
Güdel, M., & Benz, A. O. 1990, A&A, 231, 202
Güdel, M., & Zlobec, P. 1991, A&A, 245, 299
Hurford, G. J., Read, R. B., & Zirin, H. 1984, Sol. Phys., 94, 413
Karlický, M. 1984, Sol. Phys., 92, 329
Karlický, M., Sobotka, M., & Jiřička, K. 1996, Sol. Phys., 168, 375
Krucker, S., & Benz, A. O. 1994, A&A, 285, 1038
Kuijpers, J., van der Post, P., & Slottje, C. 1981, A&A, 103, 331
Ledenev, V. G. 1998, Sol. Phys., 179, 405
Li, H. G. 1987, Sol. Phys., 114, 363
Li, H. W. 1986, Sol. Phys., 104, 131
Melnikov, V. F. 1994, Radiophys. Quantum Electron., 37, 557
Melnikov, V. F., & Magun, A. 1998, Sol. Phys., 178, 153
Messerotti, M., Nonino, M., & Zlobec, P. 1985, Mem. Soc. Astron. Italiana, 56, 795
Messmer, P., & Benz, A. O. 2000, A&A, 354, 287
Mészárosová, H., Veronig, A., Zlobec, P., & Karlický, M. 2002, in Solar Variability: From Core to Outer Frontiers, ed. A. Wilson (ESA SP-506; Noordwijk: ESA), 347
Platonov, K. Yu., & Fleishman, G. D. 2001, AZh, 78, 238 (transl.: Astron. Rep., 45, 203)
Ramaty, R. 1969, ApJ, 158, 753
Sharma, R. R., & Vlahos, L. 1984, ApJ, 280, 405
Sharma, R. R., Vlahos, L., & Papadopoulos, K. 1982, A&A, 112, 377
Stähli, M., & Magun, A. 1986, Sol. Phys., 104, 117
Stepanov, A. V. 1978, AZh Pis'ma, 4, 193
Stupp, A. 2000, MNRAS, 311, 251
Vlasov, V. G., Kuznetsov, A. A., & Altyntsev, A. T. 2002, A&A, 382, 1061
Wang, S. J., Yan, Y. H., & Fu, Q. J. 2002, Sol. Phys., 209, 185
Winglee, R. M., & Dulk, G. A. 1986, Sol. Phys., 104, 93
Winglee, R. M., Dulk, G. A., & Pritchett, P. L. 1988, ApJ, 328, 809
Zlobec, P., & Karlický, M. 1998, Sol. Phys., 182, 477